Chinese Journal of
POLYMER SCIENCE

RESEARCH ARTICLE

https://doi.org/10.1007/s10118-026-3775-6
Chinese J. Polym. Sci.

Optically Active Helical Poly(phenyl isocyanide)s Bearing Achiral Benzanilide Pendants: from Controlled Synthesis to Enantioseparation Application

Jing Wang[a], Shuai Wang[a], Hai-Xu Tong[a], Na Liu[a*], and Zong-Quan Wu[b*]

[a] *The School of Pharmaceutical Sciences, Jilin University, Changchun 130021, China*
[b] *State Key Laboratory of Supramolecular Structure and Materials, College of Chemistry, Jilin University, Changchun 130012, China*

Electronic Supplementary Information

Abstract The helical structures found in biological systems, such as DNA, have inspired significant research interest in artificial helical polymers, owing to their strong potential for applications including chiral recognition and resolution, asymmetric catalysis, and other related areas. However, the preparation of single-handed helices from achiral starting materials, as well as the exploration of their chiral resolution behavior, continues to represent a considerable challenge. In this work, we present the rational design and synthesis of optically active helical poly(phenyl isocyanide)s through helix-sense selective polymerization (HSSP) of achiral phenyl isocyanide monomers, catalyzed by enantiopure Pd(II) complexes bearing *S*- or *R*-configured ligands (Pd(II)/L^S or L^R). The polymerization exhibits living and controlled characteristics, allowing for the precise modulation of molecular weights (M_n) with exceptionally narrow distributions (M_w/M_n). The resulting polymers exhibit intense optical activity and demonstrate outstanding performance in chiral recognition. Specifically, these chiral materials are utilized as a chiral stationary phase (CSP), which can separate various racemates including *α*-methylbenzylamine, cobaltic acetylacetonate, and 2-hydroxy-2-phenylacetophenone. Additionally, when applied as a chiral crystallization agent, the polymer enabled the resolution of racemic *Z*-Alanine *via* enantioselective crystallization, yielding an enantiomeric excess (*ee*) as high as 81%.

Keywords Helical polymers; Helix-sense-selective polymerization; Living polymerization; Chiral recognition; Enantiomer separation

Citation: Wang, J.; Wang, S.; Tong, H. X.; Liu, N.; Wu, Z. Q. Optically active helical poly(phenyl isocyanide)s bearing achiral benzanilide pendants: from controlled synthesis to enantioseparation application. *Chinese J. Polym. Sci.* https://doi.org/10.1007/s10118-026-3775-6

INTRODUCTION

Helices represent a crucial class of secondary structures and are commonly observed in natural systems, as exemplified by the single-stranded right-handed helices found in proteins and double-stranded right-handed helical architecture of DNA.[1,2] These helical architectures underlie a multitude of vital biological functions. Inspired by nature, researchers have developed a variety of artificial helical polymers that are widely applied in asymmetric catalysis,[3,4] chiral recognition and separation,[5–8] circularly polarized luminescence (CPL),[9–12] and enantiomer separation.[13,14] Although most helical polymers are still prepared from chiral or nonracemic monomers, the high cost of these chiral materials has motivated the development of alternative strategies that employ chiral catalysts or additives to achieve the helix-sense-selective polymerization (HSSP) of achiral monomers.[15–18] Through living/controlled helix-sense-selective polymerization, helical polymers with controlled molecular weights, narrow dispersities, and well-defined helical senses can be readily obtained.[19,20]

Although a pair of enantiomers exhibits similar physicochemical properties, their physiological and pharmacological effects may differ significantly: one enantiomer may possess therapeutic efficacy, while its mirror-image counterpart could be ineffective or even toxic.[21] Consequently, the synthesis of chiral compounds, macromolecules, and polymers with high enantiomeric purities has become a highly attractive area of research. Currently, the commonly employed methods for the artificial production of optically pure enantiomers include crystallization resolution,[22,23] chromatographic resolution,[24,25] and membrane separation.[26,27] Alternatively, column chromatography based on chiral stationary phases is now widely recognized as a highly efficient and reliable technique for isolating enantiomers in optically pure forms.[28,29] This is attributed to its superior separation efficiency, outstanding enantioselectivity, and inherent practicality and scalability, making it highly suitable for high-throughput screening applications. Currently, chiral separation materials

* Corresponding authors, E-mail: liuna606@jlu.edu.cn (N.L.)
E-mail: zqwu@jlu.edu.cn (Z.Q.W.)
Special Topic: Chirality in Polymers
Received May 28, 2026; Accepted June 8, 2026; Published online August 3, 2026

are mainly derived from natural chiral materials.[28,30–32] Given that the chiral architectures of natural polymers are not easily regulated, increasing research interest has been directed toward chiral separation materials derived from synthetic helical polymers.[33–35] Among the numerous helical polymers, polyisocyanides have attracted considerable interest in the field of functional polymers because of their unique static helical conformation, rigid alternating carbon-nitrogen double bond backbone,[36–38] and designable modifiable side chains.[39–41] Alkyne-palladium (Pd) catalysts exhibit excellent selectivity and high catalytic activity in the polymerization of isocyanide monomers, enabling efficient living polymerization under mild reaction conditions.[42] These catalysts enable the production of polyisocyanides with controlled molecular weights (M_n), narrow molecular weight distributions (M_w/M_n), and high stereoregularities.[43] In the presence of chiral ligands, alkyne-Pd(II) catalysts initiate living HSSP of achiral isocyanide monomers, thereby generating optically active helical polyisocyanides. Nevertheless, the preparation of one-handed helical polyisocyanides from a simple achiral benzanilide monomer, as well as their potential application as a chiral stationary phase for chiral recognition, has rarely been investigated.

In this study, we designed and prepared achiral monomer **1** (4-isocyano-*N*-phenylbenzamide) from commercially available materials. The HSSP of monomer **1** using chiral Pd catalysts (Pd(II)/L^S or L^R) afforded the optically active one-handed helical poly(phenyl isocyanide). Polymerization features a living character, enabling the facile synthesis of a series of polyisocyanides (*R*- or *S*-poly-**1**$_n$s) with controlled number-average molecular weights (M_n) and narrow distributions (M_w/M_n). The as-prepared polyisocyanides displayed pronounced optical activity and outstanding performance in recognizing and resolving a broad range of racemates. Upon utilization as a chiral stationary phase, these polymer materials allow for the effective separation of several racemic compounds, including *α*-methylbenzylamine, 2-hydroxy-2-phenylacetophenone, and cobaltic acetylacetonate. Furthermore, when serving as chiral crystallization agents, these helical polymers facilitated the enantioselective crystallization of racemic *Z*-alanine, delivering an enantiomeric excess (*ee*) as high as 81%. Taken together, this work provides a route for the precise construction of optically active helical polymers with good chiral resolution capabilities, starting from achiral precursors.

EXPERIMENTAL

General Considerations

All organic solvents were purchased from Sinopharm Chemical Reagent Co., Ltd., and underwent standard purification procedures prior to use. For reactions requiring anhydrous conditions, *N*,*N*-dimethylformamide (DMF), dichloromethane (CH_2Cl_2), tetrahydrofuran (THF), and triethylamine (Et_3N) were dried using standard methods and distilled prior to use. All chemical reagents were obtained from Aladdin, Sinopharm, and Sigma-Aldrich Chemical Co., Ltd., and were employed as received unless otherwise noted. NMR spectra were recorded on a Bruker 500 MHz spectrometer with chemical shifts internally referenced to tetramethylsilane or residual solvent signals. Size exclusion chromatography (SEC) was performed on a system comprising a Waters 1515 pump and Waters 2414 differential refractive index (RI) detector maintained at 40 °C. Three linear Styragel columns (HR0.5, HR3, and HR4) are connected in series. Number-average molecular weights (M_n) and polydispersity indices (M_w/M_n) were determined against polystyrene standards. Tetrahydrofuran (THF) was used as eluent at a flow rate of 0.3 mL/min. Circular dichroism (CD) spectra were acquired in a 1.0 cm quartz cuvette using a JASCO J1500 spectropolarimeter. UV-Vis absorption spectra were recorded on a Perkin-Elmer double-beam spectrophotometer at 25 °C using a 1.0 cm quartz cell. FTIR spectra were collected using a Perkin-Elmer Spectrum BX FTIR system *via* KBr pellet preparation at 25 °C. High-performance liquid chromatography (HPLC) equipped with a UV-Vis detector was performed on a Wu FENG instrument fitted with chiral columns. The alkyne palladium catalyst $ArPd(PEt_3)_2Cl$ and chiral bidentate phosphine ligands (Wei-Phos, L^R and L^S) were synthesized according to literature procedures, and their structures were confirmed by ^{1}H-NMR.[44,45] Monomer **1** was prepared according to the route shown in Scheme 1(a), based on a previously reported method, with slight modifications.[46]

Synthesis of Monomer 1

Synthesis of 4-nitro-*N*-phenylbenzamide (**2**). This compound was prepared according to the literature, albeit with certain adjustments introduced during the experimental procedure.[47] *p*-Nitrobenzoic acid (20.00 g, 119.75 mmol, 1.0 equiv.), 4-dimethylaminopyridine (DMAP, 1.62 g, 11.98 mmol, 0.1 equiv.) and 1-ethyl-3-(3-dimethylaminopropyl)carbodiimide hydrochloride (EDCI, 27.55 g, 143.70 mmol, 1.2 equiv.) were dissolved in dichloromethane (CH_2Cl_2, 200 mL). The reaction vessel was purged with nitrogen to generate an inert atmosphere. After stirring until complete dissolution, aniline (13.1 mL, 143.70 mmol, 1.022 g/mL, 1.2 equiv.) was added using a syringe, and the resulting reaction mixture was stirred overnight at room temperature. The mixture was then filtered and the filter cake was washed sequentially with saturated aqueous sodium bicarbonate solution, water, and brine, followed by drying. This afforded desired product (**2**) as a white solid (21.25 g, 73% yield) (Fig. S1 in the electronic supplementary information, ESI). ^{1}H-NMR (500 MHz, DMSO-d_6, δ, ppm): 7.23–7.06 (t, *J*=9.0 Hz, 1H), 7.48–7.31 (t, *J*=10.0 Hz, 2H), 7.86–7.72 (d, *J*=10.0 Hz, 2H), 8.27–8.11 (d, *J*=11.0 Hz, 2H), 8.47–8.32 (d, *J*=11.0 Hz, 2H), 10.64–10.52 (s, 1H).

Synthesis of 4-amino-*N*-phenylbenzamide (**3**). The target compound was synthesized according to a literature procedure with minor modifications during the experimental process.[47] Compound (**2**) was dissolved in a mixture of tetrahydrofuran (THF, 160 mL) and methanol (CH_3OH, 40 mL). Subsequently, 2.13 g of palladium on carbon (Pd/C) catalyst, corresponding to 10 wt% relative to 4-nitro-*N*-phenylbenzamide, was added to the reaction mixture. The resulting mixture was stirred under hydrogen (H_2) atmosphere for 8 h. The filter cake was washed with THF and the combined filtrate was concentrated under reduced pressure to furnish product (**3**) as a white solid (19.00 g, 90% yield). (Fig. S2 in ESI). ^{1}H-NMR (500 MHz, DMSO-d_6, δ, ppm): 9.78–9.74 (s, 1H), 7.79–7.70 (m, 4H), 7.36–7.27 (t, *J*=7.75 Hz, 2H), 7.05–7.00 (t, *J*=7.5 Hz, 1H), 6.65–6.57 (d, *J*=9.0 Hz, 2H), 5.80–5.70 (s, 2H).

Synthesis of 4-formamido-*N*-phenylbenzamide (**4**). Under a nitrogen atmosphere, formic acid (42.2 mL, 1.12 mol, 12.5

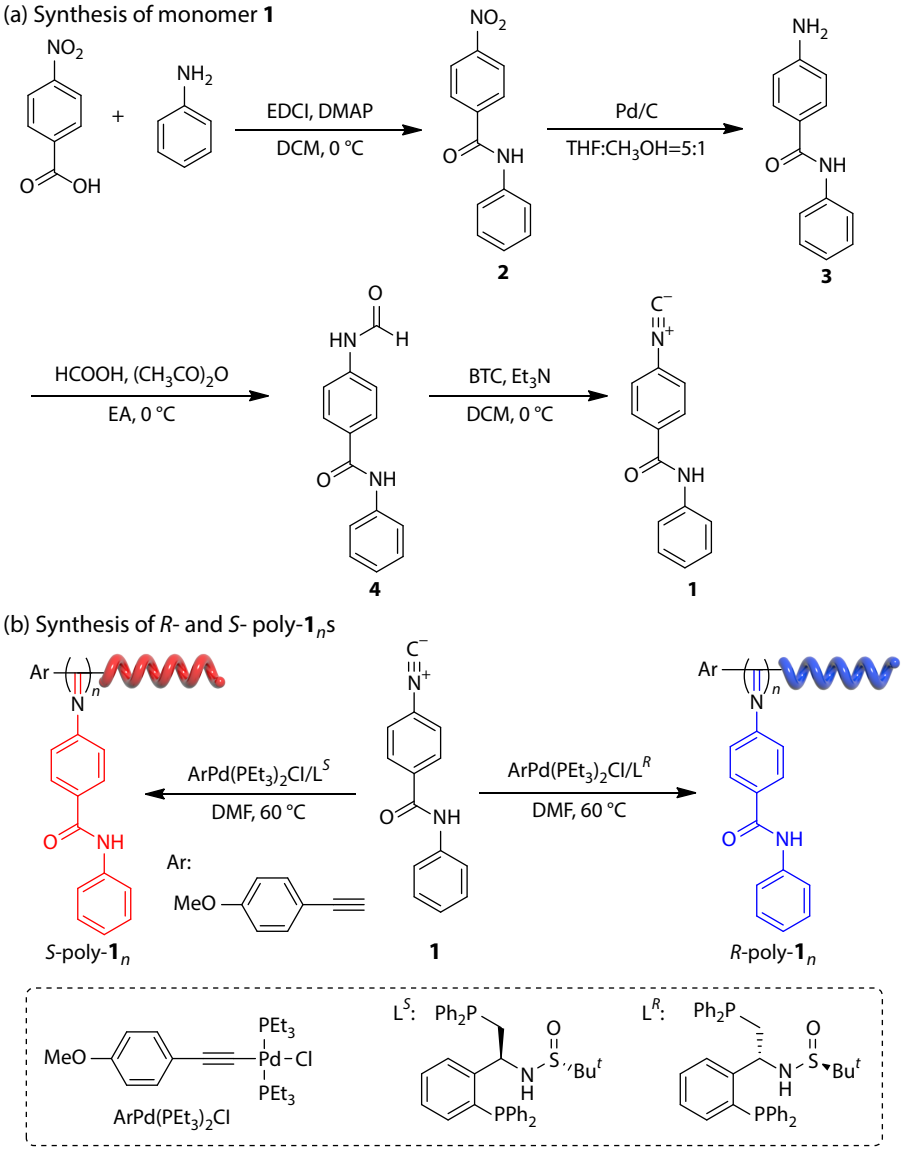

Scheme 1 Synthesis of (a) monomer **1** and (b) *R*- and *S*-poly-**1**$_n$s.

equiv.), and acetic anhydride (21.2 mL, 0.22 mol, 2.5 equiv.) were mixed and stirred at 0 °C for 3 h. Compound (**3**) was separately dissolved in ethyl acetate (EA, 200 mL). The pre-mixed formic acid/acetic anhydride mixture was then added dropwise *via* syringe to this solution at 0 °C, and the resulting mixture was stirred at the same temperature for 1 h. The reaction mixture was collected by suction filtration. The resulting solid was washed successively with water, saturated aqueous $NaHCO_3$ solution, and saturated aqueous NaCl solution and then dried to afford the product as a white solid (18.77 g, 88% yield) (Fig. S3 in ESI). ^{1}H-NMR (500 MHz, DMSO-d_6, δ, ppm): 10.63–10.36 (s, 1H), 10.26–10.05 (s, 1H), 8.40–8.30 (s, 1H), 8.03–7.89 (d, J=8.5 Hz, 2H), 7.86–7.67 (m, 2H), 7.44–7.26 (t, J=7.75 Hz, 2H), 7.17–7.00 (t, J=6.25 Hz, 1H).

Synthesis of monomer **1**.[46] Compound (**4**) (1.10 g, 4.62 mmol, 1.0 equiv.) were dissolved in dichloromethane (CH_2Cl_2, 30 mL). The flask was purged with nitrogen to establish an inert atmosphere, followed by the addition of anhydrous triethylamine (Et_3N, 3.3 mL, 23.10 mmol), and the mixture was stirred for 10 min. Bis(trichloromethyl) carbonate (BTC, 1.21 g, 4.07 mmol, 0.88 equiv.) was weighed and dissolved in 10 mL of CH_2Cl_2. The resulting solution was then added dropwise to the mixture at 0 °C, and the reaction was allowed to proceed at room temperature for 30 min under stirring. The reaction was subsequently quenched by adding water. The combined organic phase was washed successively with saturated aqueous sodium bicarbonate and saturated aqueous sodium chloride solutions, and then dried over anhydrous Na_2SO_4. After filtration and evaporation of the solvent under reduced pressure, the obtained residue was further purified using column chromatography (petroleum ether/ethyl acetate, 2/1, *V*/*V*), yielding monomer **1** as a white solid (709.0 mg, 69% yield). (Fig. S4 in ESI). Its structure was fully characterized by ^{1}H-NMR and FTIR spectra. ^{1}H-NMR (500 MHz, $CDCl_3$, δ, ppm): 7.94–7.92 (d, J=10.5 Hz, 2H), 7.53–7.51 (d, J=11.0 Hz, 2H), 7.41–7.38 (m), 7.21–7.18 (m).

https://doi.org/10.1007/s10118-026-3775-6

Preparation of the ArPd(PEt_3)$_2$Cl/L^R Catalyst. Catalysts were prepared according to a previously reported method.[44,45] A solution of as-prepared methoxyl alkynyl palladium catalyst (ArPd(PEt_3)$_2$Cl, 2.8 mg, 0.0056 mmol) in THF (0.2 mL) was treated with the phosphine ligand (L^R, 4.0 mg, 0.0067 mmol) at room temperature. The resulting mixture was stirred at room temperature for 2 h and then used directly as an initiator for polymerization of the phenyl isocyanide monomer without any further purification.

Typical Polymerization Process

Taking the synthesis of *R*-poly-**1**$_{80}$ as an example (Scheme 1b), a solution of the as-prepared ArPd(PEt_3)$_2$Cl/L^R catalyst in THF (0.20 mL, 0.028 mol/L, 0.0056 mmol) was added to a solution of monomer **1** (100.0 mg, 0.45 mmol) in DMF (0.80 mL). The resulting concentrations of monomer **1** and the catalyst were 0.45 and 0.0056 mol·L^{-1}, respectively. The initial monomer-to-catalyst feed ratio was 80/1 ([**1**]$_0$/[Pd]$_0$=80). After the polymerization mixture was stirred overnight at 60 °C, it was cooled to room temperature. Deionized water was then added to the mixture and the resulting precipitate was collected by centrifugation. The solid was subsequently washed sequentially with methanol and acetone and dried overnight under vacuum at room temperature, yielding *R*-poly-**1**$_{80}$ as a yellow solid (65.8 mg, 66% yield). (Figs. S5 and S6 in ESI). SEC: M_n=29.3 kDa, M_w/M_n=1.23. ^{1}H-NMR (500 MHz, $CDCl_3$, δ, ppm): 8.05–6.75 (m).

Kinetic Studies

A solution of the as-prepared ArPd(PEt_3)$_2$Cl/L^R catalyst in THF (0.20 mL, 0.028 mol/L, 0.0056 mmol) was introduced *via* syringe into a mixture of monomer **1** (100.0 mg, 0.45 mmol) and 1,3,5-trimethoxybenzene (25.2 mg, 0.15 mmol) in DMF (0.80 mL) ([**1**]$_0$=0.45 mol·L^{-1}, [**1**]$_0$/[Pd]$_0$=60). The polymerization mixture was stirred at 60 °C, and the reaction progress was monitored by withdrawing aliquots at regular time intervals and analyzing them using high-performance liquid chromatography (HPLC). The conversion of monomer **1** was calculated based on the peak area of unreacted monomer **1** relative to that of the internal standard 1,3,5-trimethoxybenzene on the basis of the linear calibration curve.

Typical Procedure for Enantiomeric Resolution Using *R*-poly-1$_{80}$-based CSPs

The obtained *R*-poly-**1**$_{80}$ polymer (400.0 mg) and Silica-NH_2 (2.10 g) were dispersed in THF (20 mL) and stirred at room temperature for 12 h to allow non-covalent loading of the polymer onto the surface of the amino silica gel. Subsequently, the solvent was evaporated under reduced pressure to obtain the target chiral stationary phase (CSP). The obtained CSP was then packed into a pristine stainless steel HPLC column (20 cm length × 2.0 mm i.d.) using a high-pressure slurry packing method. In a typical procedure, 2.5 g of the as-prepared *R*-poly-**1**$_{80}$@SiO_2 material was suspended in a mixture of *n*-hexane and isopropanol (90/10, *V*/*V*) followed by ultrasonication for 5 min to form a homogeneous slurry. The slurry was then packed into an empty column using the same solvent mixture (*n*-hexane/isopropanol, 90/10, *V*/*V*) as the displacement liquid under a constant pressure of 30 MPa, which was maintained for 5 min. The packed *R*-poly-**1**$_{80}$@SiO_2 column was subsequently connected to the HPLC system and preconditioned with a mobile phase (*n*-hexane/isopropanol, 90/10, *V*/*V*) at a flow rate of 0.5 mL·min^{-1} until a stable baseline was achieved. Prior to injection, all sample solutions were filtered through a 0.22 μm membrane filter. The injection volumes ranged from 20 μL to 30 μL. Unless otherwise specified, all chromatographic separations were conducted at room temperature using a mobile phase composed of *n*-hexane and isopropanol (97/3, *V*/*V*), delivered at a flow rate of 0.2 mL·min^{-1}. The detection wavelength was set at 254 nm. Dead time was determined using 1,3,5-trimethoxybenzene.

Typical Procedure for Enantioselective Crystallization

The crystallization experiment was conducted in a supersaturated solution of racemic *Z*-Alanine prepared in a mixture of methanol and deionized water. Specifically, racemic *Z*-Alanine (100.0 mg) was added to deionized water (10 mL). The mixture was then heated to 40 °C, and methanol was slowly added dropwise until complete dissolution of the racemic mixture was achieved. Subsequently, approximately 10.0 mg of *R*-poly-**1**$_{80}$ was added to the supersaturated solution, followed by ultrasonication for approximately 30 min. Under these conditions, *R*-poly-**1**$_{80}$ remained suspended as solid particles, while racemic *Z*-Alanine remained fully dissolved in the liquid phase. The resulting dispersion was allowed to cool naturally to room temperature (approximately 25 °C). After standing for an appropriate period, needle-like crystals gradually formed. The obtained crystals were collected by filtration, washed with cold methanol, and dried under vacuum at ambient temperature to yield optically active *Z*-*D*-Alanine. The enantiomeric excess (*ee*) of the resulting *Z*-*D*-Alanine crystals was determined by comparing their circular dichroism (CD) intensity with that of commercially available enantiopure *Z*-*D*-Alanine.

RESULTS AND DISCUSSION

Synthesis and Characterization

Polyisocyanides were successfully synthesized and their chemical structures were confirmed by ^{1}H-NMR and Fourier-transform infrared (FTIR) spectroscopy (Schemes 1a and 1b, Figs. S5 and S6 in ESI). Chiral ligand (L^R)/Pd(II) catalysts were prepared following the procedures previously reported by our group.[19,48–50] The resulting catalyst solution was directly used for isocyanide polymerization without additional isolation or purification steps (Scheme 1b). Initially, polymerization of the achiral phenyl isocyanide monomer **1** was conducted in DMF at 60 °C under the conditions of [**1**]$_0$/[Pd]$_0$=80/1 and [**1**]$_0$=0.45 mol·L^{-1}. Size exclusion chromatography (SEC) analysis of the resulting *R*-poly-**1**$_n$s samples with varying theoretical degrees of polymerization (DP = 20, 40, 60, 80, 100) exhibited unimodal elution profiles (Fig. 1a). The number-average molecular weights (M_n) of *R*-poly-**1**$_n$s correlated linearly with the monomer-to-Pd feeding ratios, indicating that polymerization proceeded in a controlled/living manner. All the polymers displayed narrow dispersities (M_w/M_n < 1.26 (Fig. 1b, Table 1). To gain deeper mechanistic insights, the kinetics of polymerization initiated by the L^R/Pd(II) catalyst ([**1**]$_0$/[Pd]$_0$=60) were monitored by SEC and HPLC. The M_n values of the isolated polymers increased linearly with monomer conversion, while M_w/M_n remained low throughout the reaction (Fig. 1c and Fig. S7 in ESI). A monomer conversion of 95% was achieved within 2.5 h, indicating near-complete polymerization (Fig. 1d and Fig. S8 in ESI). Kinetic analysis revealed that the polymerization followed a

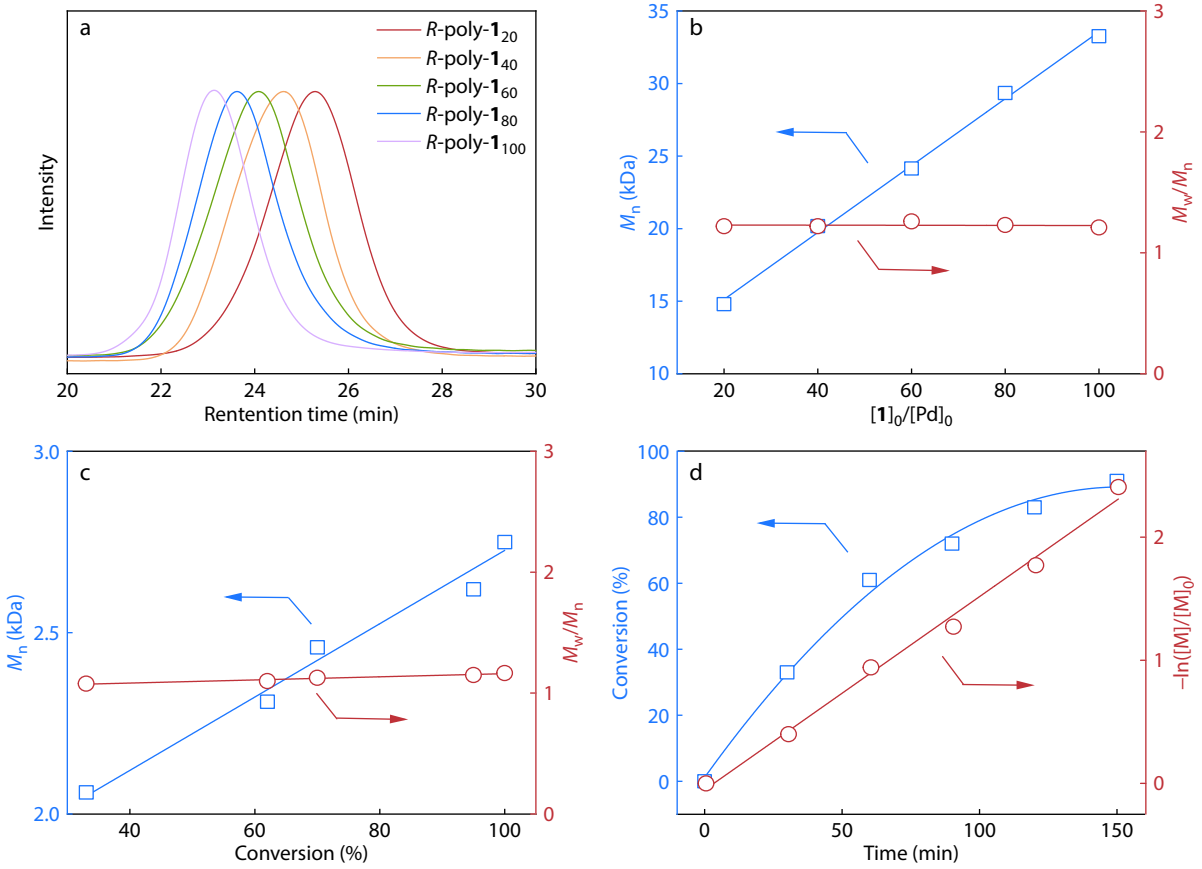

Fig. 1 (a) SEC curves for *R*-poly-**1**$_n$s synthesized with different initial feed ratios of monomer to catalyst; (b) Plots of M_n and M_w/M_n values for *R*-poly-**1**$_n$s versus the initial feed ratio of monomer to catalyst; (c) Plots of M_n and M_w/M_n versus the conversion of monomer **1**; (d) Plot of monomer conversion as a function of the polymerization time and first-order kinetic plot for the polymerization of monomer **1** initiated by Pd(II) catalyst.

Table 1 Polymerization results for monomer 1 initiated by chiral Pd(II) catalysts.

Run	Polymer [a]	M_n [b] (kDa)	M_w/M_n [b]	Yield [c]	$\Delta\varepsilon$ [d] (L·mol^{-1}·cm^{-1})
1	*R*-poly-**1**$_{20}$	14.8	1.22	67%	1.90
2	*R*-poly-**1**$_{40}$	20.2	1.22	73%	3.62
3	*R*-poly-**1**$_{60}$	24.1	1.26	71%	5.79
4	*R*-poly-**1**$_{80}$	31.6	1.25	66%	7.54
5	*R*-poly-**1**$_{100}$	31.3	1.21	65%	7.60
6	*S*-poly-**1**$_{80}$	30.8	1.24	75%	−7.56

[a] The polymers were prepared following the Scheme 1. [b] The M_n and M_w/M_n values were determined by SEC using polystyrene standards. [c] Isolated yields. [d] $\Delta\varepsilon$ values were obtained from CD recorded in THF at room temperature.

first-order reaction mechanism, with an apparent rate constant of 1.57×10^{-2} min^{-1} (Fig. 1d). Collectively, these results support a controlled/living polymerization mechanism for the isocyanide monomers. Meanwhile, as DP increased, the solubility of the resulting polymer in common solvents decreased. Therefore, the DP was limited to a maximum of 80 in this study.

Optical Properties

After successfully synthesizing a series of poly(phenyl isocyanide) samples with targeted number-average molecular weights and narrow dispersities, their optical activities were systematically evaluated using circular dichroism (CD) and UV-Vis spectroscopy. Notably, although monomer **1** itself is achiral, the resulting polymers, denoted as *R*-poly-**1**$_n$ (n=20, 40, 60, 80, and 100), all exhibited significant optical activity. As shown in Fig. 2(a), the maximum positive Cotton effect was clearly observed at approximately 364 nm, which corresponds to the characteristic absorption band of the poly(phenyl isocyanide) backbone, indicating that the polymer backbone predominantly adopts a right-handed helical conformation. Further analysis revealed that the absolute $\Delta\varepsilon_{364}$ value of *R*-poly-**1**$_n$s increased with increasing molecular weight and reached a plateau at n=80.[51] When the number-average molecular weight reached 31.3 kDa, the maximum absolute $\Delta\varepsilon$ value was determined to be 7.60 L·mol^{-1}·cm^{-1} (Table 1). Collectively, these trends confirm the formation of a stable helical structure. The increase in helicity with increasing molar mass originates primarily from the "terminal defect effect." At low molar masses, the nonhelical regions at the chain ends account for a relatively high proportion, resulting in low net helicity. As the chain grows, the proportion of

https://doi.org/10.1007/s10118-026-3775-6

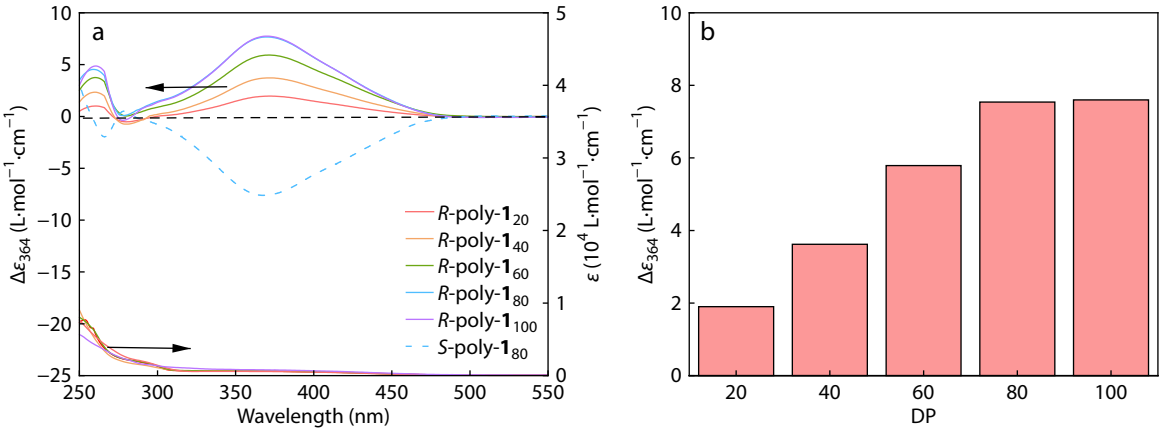

Fig. 2 (a) CD and absorption spectra of *R*-poly-**1**$_n$s (n=20, 40, 60, 80, 100) in THF at room temperature; (b) Plot of CD intensity of *R*-poly-**1**$_n$s in THF at room temperature.

regular helical segments increases, and the terminal defects become diluted, leading to a gradual enhancement in helicity that eventually reaches a plateau. It was revealed that the CD intensity of helical polyisocyanides reached a plateau when DP reached about 80 (Fig. 2). Because polyisocyanides possess a stable helical conformation, further increasing the DP does not enhance the chiral separation efficiency.

To investigate whether the helix-sense-selective polymerization of achiral monomer **1** was initiated by the chiral Pd(II) complex, polymerization of monomer **1** was carried out under identical experimental conditions using the enantiomeric L^S/Pd(II) complex as the catalyst. The results indicate that this polymerization process exhibited both living and controlled characteristics. Circular dichroism (CD) measurements revealed that the as-prepared *S*-poly-**1**$_{80}$ displayed a maximum negative Cotton effect at approximately 364 nm, which was nearly mirror-imaged compared to that of *R*-poly-**1**$_{80}$ (Fig. 2b), suggesting the predominant formation of a left-handed helical conformation. Given that both *S*-poly-**1**$_n$s and *R*-poly-**1**$_n$s were synthesized from the same achiral monomer under identical experimental conditions, the mirror-image relationship in their Cotton effects can be reasonably ascribed to the chiral induction exerted by the chiral catalyst during polymerization. These findings further validated the helix-sense-selective nature of the living/controlled polymerization of the achiral phenyl isocyanide monomer, catalyzed by a chiral Pd(II) complex. The helical stability of the resulting *R*-poly-**1**$_{80}$ was evaluated using CD and UV-Vis analyses conducted at various temperatures and in different solvents. When the solution temperature was increased from 25 °C to 80 °C in DMF, only minor changes were observed in the CD and UV-Vis spectra of *R*-poly-**1**$_{80}$, indicating the preservation of a stable helical conformation even at elevated temperatures (Fig. S9 in ESI). Similarly, the CD and UV-Vis spectra of *R*-poly-**1**$_{80}$ remained largely unchanged in organic solvents of varying polarities, including THF, CH_2Cl_2, $CHCl_3$, and MeCN (Fig. S10 in ESI), further corroborating the robustness of the helical structure. Moreover, a linear correlation was observed between the polymer concentration and both the CD and UV-Vis absorption intensities, suggesting that the optical activity of *R*-poly-**1**$_{80}$ arises from the helical conformation of the polyisocyanide backbone rather than from intermolecular aggregation in the solution (Fig. S11 in ESI). The interesting high stability of the helical conformation of these polymers may arise from the synergistic effect of the rigid polyisocyanide backbone, which imposes a high-energy barrier for helix inversion. Moreover, hydrogen bonding interactions between the amide pendants provided additional stabilization energy (Fig. S6 in ESI).

Chiral Recognition and Resolution Ability

As the obtained poly(phenyl isocyanide)s were optically active, they were expected to possess chiral recognition and separation capabilities. A chiral stationary phase (CSP) for high-performance liquid chromatography (HPLC) was prepared by coating polyisocyanides onto silica gel. The chiral separation performance of this CSP toward five racemic mixtures (A–E) was evaluated using HPLC with a UV detector (Fig. 3a). The separation efficiency was assessed based on the retention time [$k_1 = (t_1 - t_0)/t_0$] and the separation factor [$\alpha = (t_2 - t_0)/(t_1 - t_0)$]. Among the prepared polyisocyanide-based CSPs, the *R*-poly-**1**$_{80}$-based CSP exhibited excellent separation performance (α=2.28–3.29) (Table 2) and successfully resolved racemates A, B, and E into pure enantiomers (Figs. 3b, 3c and Figs. S12–S14 in ESI). For example, when employed for the separation of racemate A using *n*-hexane/isopropanol = 97/3 (*V*/*V*) as the mobile phase at a flow rate of 0.2 mL·min^{-1}, two enantiomeric peaks with distinct retention times were clearly observed, with k_1=4.51, k_2=10.28, and a separation factor (α) of 2.28. These results demonstrate that the *R*-poly-**1**$_{80}$-based CSP achieved baseline separation of racemate A. The superior performance of *R*-poly-**1**$_{80}$-based CSP can be attributed to two factors. First, the stable chiral helical structure of the polyisocyanide backbone provides a favorable recognition environment for chiral molecules. Second, the amide groups in the side chains can form hydrogen bonds with analyte molecules. The intermolecular π–π interaction between the analyte and benzyl pendants of helical *R*-poly-**1**$_{80}$ further enhanced the enantiomer recognition capability. The synergistic effect of these factors endows CSP with excellent chiral resolution performance. Notably, *R*- and *S*-poly-**1**$_n$s were insoluble in both *n*-hexane and isopropanol. Thus, the coated polymers were barely dissolved and washed out by the *n*-hexane/isopropanol eluent.

Among the five racemates investigated in this work, racemates A, B, D, and E could form hydrogen bonds with the

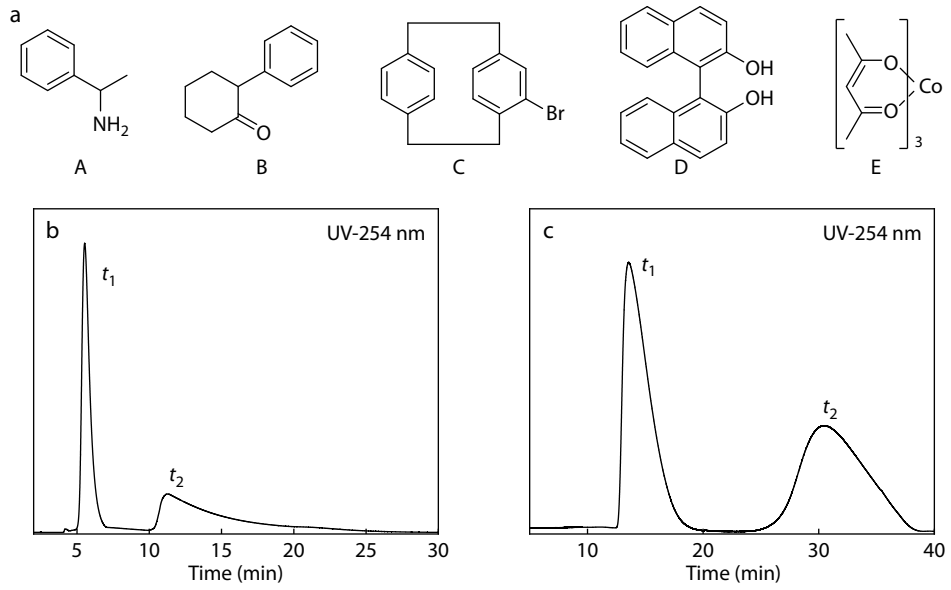

Fig. 3 (a) Structures of selected racemates (A–E); HPLC traces for the enantioseparation of A (b), B (c) using *R*-poly-**1**$_{80}$-based CSPs with UV detectors.

Table 2 Chiral resolution results of racemates (A–E) on CSPs consisting of *R*-poly-**1**$_{80}$.

Run	Racemate	*R*-poly-**1**$_{80}$ CSP [a]		
		k_1	k_2	α
1	A [b]	4.51	10.28	2.28
2	B [b]	12.58	29.50	2.34
3	C [b]	26.00	–	1.00
4	D [b]	41.89	71.07	1.70
5	E [b]	23.44	77.05	3.29

[a] Columns: 20 × 0.20 (i.d.) cm; temperature: 25°C. The signs in parentheses represent the Cotton effect signs at 254 nm of the first-eluted enantiomers. [b] Eluent: *n*-hexane/2-propanol (97/3, *V*/*V*), flow rate: 0.2 mL·min^{-1}.

amide groups of the *R*-poly-**1**$_{80}$ side chains, and enantioseparation was achieved because of the difference in binding affinity between the *R* and *S* configurations toward the CSP. In contrast, racemate C lacked hydrogen-bonding interaction sites and, therefore, did not exhibit effective chiral recognition. Specifically, racemate D possesses two rigid naphthalene ring planes that can generate strong π-π stacking with helical polyisocyanide pendants. Meanwhile, its two hydroxyl groups can form more stable hydrogen bonds with the stationary phase, as indicated by the FTIR analysis (Fig. S15 in ESI). These multiple interactions prolong the retention time of the chiral columns. Racemate E, as a metal complex, can undergo coordination interactions with the stationary phase, resulting in stronger adsorption and, consequently, a longer retention time.

In addition to separation, the chiral recognition ability of *R*-poly-**1**$_{80}$ was further exploited for enantioselective crystallization. To verify this, *R*-poly-**1**$_{80}$ was selected as the chiral inducer for the enantioselective crystallization of *Z*-Alanine racemate. An oversaturated solution of *Z*-Alanine (100.0 mg in 8 mL of methanol/water) was maintained at 25 °C in the presence of *R*-poly-**1**$_{80}$ (10.0 mg), whereupon needle crystals

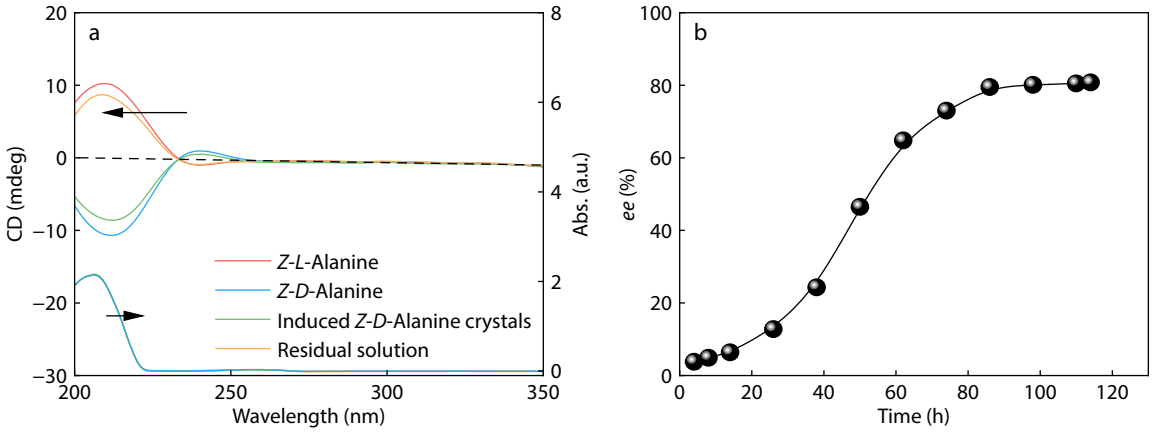

Fig. 4 (a) CD and UV-Vis spectra of the crystals and residual solution of the enantioselective crystallization of *Z*-Alanine racemates induced by *R*-poly-**1**$_{80}$ and enantiopure *L*- and *D*-threonine in aqueous solutions; (b) Plot of *ee* (%) value for the residual solution with crystallization time for the enantioselective crystallization of threonine induced by *R*-poly-**1**$_{80}$.

https://doi.org/10.1007/s10118-026-3775-6

formed gradually. These crystals displayed a negative Cotton effect at about 210 nm, indicating preferential crystallization of *Z*-*D*-Alanine. Conversely, the residual mother liquor exhibited a positive Cotton effect, indicating the enrichment of *Z*-*L*-Alanine (Fig. 4a). This is because during the crystallization process, the helical polymer *R*-poly-$\mathbf{1}_{80}$, by virtue of its stable helical structure, selectively nucleated *Z*-*D*-alanine. This process led to the preferential adsorption of *Z*-*D*-alanine at the interface of the helical polymer, resulting in progressive enrichment of *Z*-*L*-alanine in the solution. Ultimately, enantioselective macroscopic crystallization with *R*-poly-$\mathbf{1}_{80}$ as the nucleation site is achieved. The enantiomeric excess (*ee*) of the crystals, as determined by CD, increased with crystallization time, ultimately reaching 81% (Fig. 4b).

CONCLUSIONS

In summary, optically active helical poly(phenyl isocyanide)s were readily synthesized *via* the living helix-sense-selective polymerization of achiral isocyanides using chiral Pd(II) complexes as catalysts. A series of helical poly(phenyl isocyanide)s with the anticipated number-average molecular weights (M_ns) and narrow molecular weight distributions (M_w/M_ns) were successfully obtained. The resulting polymers adopted stable helical conformations with a preferred handedness induced by chiral Pd(II) catalysts, and the direction of the helix was dictated by the chirality of the corresponding chiral ligands. Moreover, these optically active poly(phenyl isocyanide)s exhibited exceptional chiral recognition and resolution capabilities, serving both as chiral stationary phases and crystallization inducers. This study not only provides a strategy for the precise synthesis of optically active helical polymers from achiral precursors but also offers chiral materials with considerable potential for enantiomer separation.

Conflict of Interests

The authors declare no interest conflict.

Electronic Supplementary Information

Electronic supplementary information (ESI) is available free of charge in the online version of this article at http://doi.org/10.1007/s10118-026-3775-6.

Data Availability Statement

The data supporting the findings of this study are available from the corresponding author upon reasonable request.

ACKNOWLEDGMENTS

This work was financially supported by the National Natural Science Foundation of China (Nos. 52573008, 22571117 and 52273006), Major Research Plan of the National Natural Science Foundation of China (Nos. 92256201 and 92356302), and the Science and Technology Development Plan of Jilin Province (No. 20240101181JC).

REFERENCES

1 Lechner, V. M.; Nappi, M.; Deneny, P. J.; Folliet, S.; Chu, J. C. K.; Gaunt, M. J. Visible-light-mediated modification and manipulation of biomacromolecules. *Chem. Rev.* **2022**, *122*, 1752−1829.
2 Cao, J.; Zaremba, O. T.; Lei, Q.; Ploetz, E.; Wuttke, S.; Zhu, W. Artificial bioaugmentation of biomacromolecules and living organisms for biomedical applications. *ACS Nano* **2021**, *15*, 3900−3926.
3 Ikai, T.; Ando, M.; Ito, M.; Ishidate, R.; Suzuki, N.; Maeda, K.; Yashima, E. Emergence of highly enantioselective catalytic activity in a helical polymer mediated by deracemization of racemic pendants. *J. Am. Chem. Soc.* **2021**, *143*, 12725−12735.
4 Zhou, L.; He, K.; Liu, N.; Wu, Z.-Q. Recent advances in asymmetric organocatalysis based on helical polymers. *Polym. Chem.* **2022**, *13*, 3967−3974.
5 Zhou, Y.; Zhang, C.; Huang, J.; Liu, L.; Bai, J.; Li, J.; Satoh, T.; Okamoto, Y. Positive synergy between the helical poly (phenylacetylene) backbones and the helical *L*-proline oligopeptide pendants for enhanced enantioseparation properties. *Anal. Chem.* **2024**, *96*, 2078−2086.
6 Tilottama, B.; Vijayakrishna, K. Synthetic helical polymers: an overview on synthesis and their chiral separation efficiency. *Eur. Polym. J.* **2024**, *213*, 113071.
7 Tilottama, B.; Vijayakrishna, K. Polymers bearing covalently linked chiral proline-based pendants: induction of a highly stable helical sense that mimics double-stranded helical morphology and their chiral resolution ability. *Macromolecules* **2024**, *57*, 3212−3222.
8 Ikai, T.; Matsumoto, T.; Takeda, S.; Oki, K.; Yashima, E. Tunable synthesis of one-handed helical ladder polymers with a helical cavity or helical grooves for advanced chiral recognition. *Macromolecules* **2025**, *58*, 6943−6952.
9 Ikai, T. The dawn of chiral material development using saccharide-based helical polymers. *Polym. J.* **2017**, *49*, 355−362.
10 Zhao, J.; Shi, S.; Zhang, X.; Liu, D.; Song, F.; Cheng, Y.; Li, F. Circularly polarized luminescence pyrene materials: from design to applications. *Coord. Chem. Rev.* **2026**, *548*, 217173.
11 Li, Z.-Q.; Zhang, D.-C.; Wang, H.-X.; Li, M.; Jiang, W.; Zhang, Y.; Huang, Z.; Zhong, H.; Wei, N.-X.; Dong, X.; Zhao, W.; Ji, H.; Yuan, L.; Zhou, Z.; Zhang, J.; Zhang, M.; Li, S.; Li, L.; Gu, Z.-G.; Qiu, Z.; Zhao, B.; Wang, Z.; Ma, X.; Cheng, Y.; Deng, J.; Zhang, J.; Zang, S.-Q.; Long, G.; Duan, P.; Chen, C.-F.; Zheng, Y.-X.; Zhao, Y.-S.; Luo, J.; Chen, R.; Zhuang, T.; Zhong, Y.-W.; Tang, B.-Z.; Liu, M. Circularly polarized luminescence: materials, photophysics, devices, and applications. *Sci. China Chem.* **2026**, *69*, 2127−2192.
12 Li, T.; Zhu, X.; Ouyang, G.; Liu, M. Circularly polarized luminescence from chiral macrocycles and their supramolecular assemblies. *Mater. Chem. Front.* **2023**, *7*, 3879−3903.
13 Zhao, B.; Lin, J.; Deng, J.; Liu, D. Seed-surface grafting precipitation polymerization for preparing microsized optically active helical polymer core/shell particles and their application in enantioselective crystallization. *Macromol. Rapid Commun.* **2018**, *39*, 1800072.
14 Huang, S.; Teraguchi, M.; Kaneko, T.; Aoki, T. Preparation and enantioselective permeation of polymer membranes containing one-handed helical channels. *ACS Appl. Polym. Mater.* **2024**, 62049−62053.
15 Zhang, Y.; Deng, J.; Pan, K. Chiral helical polymer nanomaterials with tunable morphology: prepared with chiral solvent to induce helix-sense-selective precipitation polymerization. *Macromolecules* **2018**, *51*, 8878−8886.
16 Zou, H.; Wu, Q. L.; Zhou, L.; Hou, X. H.; Liu, N.; Wu, Z. Q. Chiral recognition and resolution based on helical polymers. *Chinese J.*

Graphical Abstract

Optically Active Helical Poly(phenyl isocyanide)s Bearing Achiral Benzanilide Pendants: from Controlled Synthesis to Enantioseparation Application

Jing Wang, Shuai Wang, Hai-Xu Tong, Na Liu, and Zong-Quan Wu

Jilin University

Optically active helical poly(phenyl isocyanide)s bearing achiral benzanilide pendants were prepared *via* helix-sense-selective living polymerization. The resulting polymers, featuring controlled molecular weights and narrow distributions, exhibit excellent chiral recognition abilities, enabling their use as chromatographic enantioseparation and enantioselective crystallization materials.

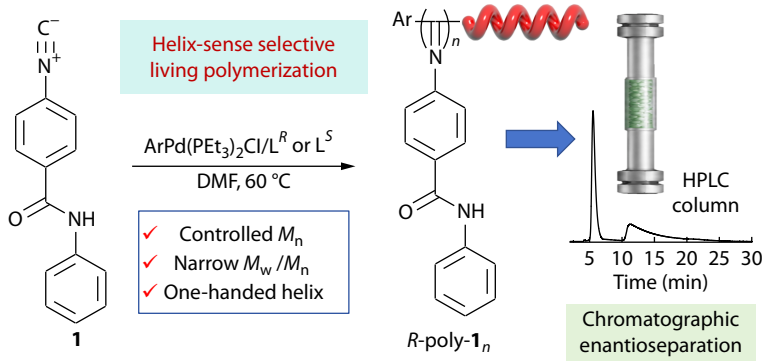

Chinese J. Polym. Sci., 2026 *https://doi.org/10.1007/s10118-026-3775-6*

Polym. Sci. **2021**, *39*, 1521–1527.
17 Zhao, B.; Deng, J. Emulsion polymerization of acetylenics for constructing optically active helical polymer nanoparticles. *Polym. Rev.* **2017**, *57*, 119–137.
18 Liu, L.; Zang, Y.; Jia, H.; Aoki, T.; Kaneko, T.; Hadano, S.; Teraguchi, M.; Miyata, M.; Zhang, G.; Namikoshi, T. Helix-sense-selective polymerization of achiral phenylacetylenes and unique properties of the resulting *cis*-cisoidal polymers. *Polym. Rev.* **2017**, *57*, 89–118.
19 Xue, Y. X.; Zhu, Y. Y.; Gao, L. M.; He, X. Y.; Liu, N.; Zhang, W. Y.; Yin, J.; Ding, Y.; Zhou, H.; Wu, Z. Q. Air-stable (phenylbuta-1, 3-diynyl)palladium (II) complexes: highly active initiators for living polymerization of isocyanides. *J. Am. Chem. Soc.* **2014**, *136*, 4706–4713.
20 Zong, Y.; Gao, R.-T.; Liu, N.; Lei, S.; Li, Z.-T.; Wu, Z.-Q. Precise synthesis of telechelic rodlike polyisocyanides: versatile building blocks for fabricating polymer frameworks with controllable pore-apertures. *Chem. Sci.* **2026**, *17*, 255–264.
21 Almeida, A. S.; Santos, R. M. G.; de Pinho, P. G.; Remião, F.; Fernandes, C. Exploring the impact of chirality of synthetic cannabinoids and cathinones: a systematic review on enantioresolution methods and enantioselectivity studies. *Int. J. Mol. Sci.* **2025**, *26*, 6471.
22 Wang, Z.; Ye, X.; Chen, Y.; Liu, Y.; Xie, S.; Tao, Y.; Zhang, J.; Wan, X. Stereoselective crystallization of chiral pharmaceuticals aided by cellulose derivatives through helical pattern matching. *Chem. Eur. J.* **2024**, *30*, e202401550.
23 Wang, Z.; Liu, Y.; Chen, Y.; Zhang, J.; Ye, X.; Wan, X. Direct crystallization resolution of racemic compounds *via* recognition of homochiral periodic structures using polymeric additives. *Cryst. Growth Des.* **2025**, *25*, 5275–5283.
24 Francotte, E. R. Enantioselective chromatography as a powerful alternative for the preparation of drug enantiomers. *J. Chromatogr. A* **2001**, *906*, 379–397.
25 Dong, H.; Zheng, M.; Ou, Y.; Zhang, C.; Liu, L.; Li, J.; Yang, X. A chiral stationary phase coated by surface molecularly imprinted polymer for separating 1,1′-binaphthalene-2,2′-diamine enantiomer by high performance liquid chromatography. *J. Chromatogr. A* **2015**, *1376*, 172–176.
26 Ma, X.; Wang, M.; Li, W.; Qi, J.; Tu, S.; Zhang, L.; Wang, K. Y.; Fu, Y.; Han, Z.; Wu, X.; Zhou, H. C.; Zhu, C. An amino-acid-derived metal–organic framework with large pores for unspecific enantioseparation. *J. Am. Chem. Soc.* **2026**, *148*, 12024–12032.
27 Lin, Y.; Li, S.; Yang, H.; Mo, Q.; Lyu, S.; Luo, H.; Yang, F.; Li, X.; Xia, F. Photoresponsive and reusable chiral metal–organic framework hybrid nanochannel membrane for drug enantioseparation. *ACS Appl. Mater. Interfaces* **2026**, *18*, 8589–8598.
28 Shen, J.; Okamoto, Y. Efficient separation of enantiomers using stereoregular chiral polymers. *Chem. Rev.* **2016**, *116*1094-1138
29 Zhang, C.; Liu, L.; Okamoto, Y. Enantioseparation using helical polyacetylene derivatives. *TrAC Trends Anal. Chem.* **2020**, *123*, 115762.
30 Aboul-Enein, H. Y.; Kannappan, V.; Kanthiah, S. Polysaccharide and cyclodextrin-based monolithic chiral stationary phases and its application to chiral separation. *Comb. Chem. High Throughput Screen.* **2023**, *26*, 2583–2597.
31 Dhekale, N. H.; Gunjal, D. B.; Gore, A. H.; Komaravolu, Y.; Bindu, K. H.; Kolekar, G. B. Stereoselective HPLC separation of alvimopan on cellulose-based immobilized polysaccharide as a chiral stationary phase. *Chirality* **2018**, *30*, 982–987.

32 Chu, B.; Song, F.; Zou, H. Controlled synthesis of β-cyclodextrin-based starlike helical poly (phenyl isocyanide) and its application in chiral resolution. *Carbohydr. Polym.* **2025**, *357*, 123456.
33 Yuan, S.; Zhao, L.; Wang, F.; Tan, L.; Wu, D. Recent advances of optically active helical polymers as adsorbents and chiral stationary phases for chiral resolution. *J. Sep. Sci.* **2023**, *46*, 2300363.
34 Shi, G.; Dai, X.; Xu, Q.; Shen, J.; Wan, X. Enantioseparation by high-performance liquid chromatography on proline-derived helical polyacetylenes. *Polym. Chem.* **2021**, *12*, 242−253.
35 Salikolimi, K.; Praveen, V. K.; Sudhakar, A. A.; Yamada, K.; Horimoto, N. N.; Ishida, Y. Helical supramolecular polymers with rationally designed binding sites for chiral guest recognition. *Nat. Commun.* **2020**, *11*, 2311.
36 Schwartz, E.; Koepf, M.; Kitto, H. J.; Nolte, R. J. M.; Rowan, A. E. Helical poly (isocyanides): past, present and future. *Polym. Chem.* **2011**, *2*, 33−47.
37 Nolte, R. J. M. Helical poly (isocyanides). *Chem. Soc. Rev.* **1994**, *23*, 11.
38 Du, X. H.; Du, Y. N.; Ye, C. C.; Dai, S. S.; Li, G. W.; Xu, L. Synthesis of double-stranded polymers based on stereoregular rigid helical poly (phenyl isocyanide)s. *Polym. Chem.* **2026**, *17*, 690−696.
39 Wang, C.; Deng, R.; Weck, M. Orthogonal supramolecular assemblies using side-chain functionalized helical poly (isocyanide)s. *Macromolecules* **2023**, *56*, 3507−3516.
40 Xu, A.; Hu, G.; Hu, Y.; Zhang, X.; Liu, K.; Kuang, G.; Zhang, A. Remarkable structure effects on chiroptical properties of polyisocyanides carrying proline pendants. *Chem. Asian J.* **2013**, *8*, 2003−2014.
41 Deng, R.; Wang, C.; Milton, M.; Tang, D.; Hollingsworth, A. D.; Weck, M. Side-chain functionalized supramolecular helical brush copolymers. *Polym. Chem.* **2021**, *12*, 4916−4923.
42 Liu, N.; Zhou, L.; Wu, Z. Q., Alkyne-palladium (II)-catalyzed living polymerization of isocyanides: an exploration of diverse structures and functions. *Acc. Chem. Res*. **2021,** *54*, 3953–3967.
43 Li, Y.; Kang, S. M.; Shi, G.; Chen, Y.-F.; Li, B. W.; Zhang, J.; Wan, X. H. Synthesis of proline-derived helical copolyacetylenes as chiral stationary phases for HPLC enantioseparation. *Chinese J. Polym. Sci.* **2025**, *43*, 61−69.
44 Zhou, L.; Xu, X.-H.; Jiang, Z.-Q.; Xu, L.; Chu, B.-F.; Liu, N.; Wu, Z.-Q. Selective synthesis of single-handed helical polymers from achiral monomer and a mechanism study on helix-sense-selective polymerization. *Angew. Chem. Int. Ed.* **2021**, *60*, 806−812.
45 Sun, Z.-Z.; Zhang, Y.-N.; Qiu, H.-Y.; Lu, X.-T.; Ren, L.-X.; Shen, L.-F.; Li, W.; Zhang, A. Synthesis of helical poly (phenylacetylene)s carrying dendritic pendants with varied branching densities through polymerization in different solvents. *Chinese J. Polym. Sci.* **2023**, *41*, 1543−1554.
46 Brunelli, F.; Ceresa, C.; Aprile, S.; Coppo, L.; Castiglioni, B.; Bosetti, M.; Fracchia, L.; Tron, G. C. Isocyanides in med chem: a scaffold hopping approach for the identification of novel 4-isocyanophenylamides as potent antibacterial agents against methicillin-resistant Staphylococcus aureus. *Eur. J. Med. Chem.* **2023**, *246*, 114950.
47 Klos, J.; Wurm, F.; König, H. M.; Kilbinger, A. F. M. Automated large-scale synthesis of supramolecular oligo (*p*-benzamide) block copolymers. *Macromolecules* **2007**, *40*, 7827−7833.
48 Gao, R.-T.; Kang, S.-M.; Zong, Y.; Li, T.-T.; Liu, N.; Wu, Z.-Q. Polymer frameworks with controllable pore size and chirality for enantioseparation of racemates with different sizes and chiralities. *CCS Chem*. **2026**, doi: 10.31635/ccschem.026.202506825.
49 Gao, R.-T.; Ma, Y.-Y.; Xu, Y.; Wang, J.; Liu, N.; Liu, F.; Wu, Z.-Q. Eugenol-based optically active helical polymers: from controlled synthesis to post-polymerization modification and chiral recognition. *Sci. China Mater.* **2026**, *69*, 2574−2582.
50 Gao, B. R.; Wu, Y. J.; Xu, L.; Zou, H.; Zhou, L.; Liu, N.; Wu, Z.-Q. Synthesis of optically active helical polycarbenes through helix-sense-selective polymerization strategy and their application in chiral separation. *ACS Macro Lett*. **2022**, 11785−11791.
51 Nath, G. Y.; Samal, S.; Park, S.-Y.; Murthy, C. N.; Lee, J.-S. Induction of helicity in poly (*n*-hexyl isocyanate) with terminal chiral residues. *Macromolecules* **2006**, *39*, 5965−5966.